

An Ultra-Wideband Baseband Front-End

Fred S. Lee, David D. Wentzloff and Anantha P. Chandrakasan

MIT Microsystems Technology Laboratory, Cambridge, MA, 02139, USA

Abstract — A 900MHz bandwidth front-end with a -100dB/decade roll-off for a baseband pulse-based BPSK ultra-wideband transceiver is designed and tested in 1.8V $0.18\mu\text{m}$ CMOS. Trade-offs in noise figure (NF) and voltage gain within broadband power-matched and un-matched (voltage-boosted) conditions of the front-end are discussed. The front-end achieves 38dB of gain and 10.2dB of average NF in the power-matched case, and 42dB of gain and 7.9dB of average NF in the un-matched case. Theory and measurements of the matching techniques and microwave design parameters upon NF and UWB signal to sinusoidal interferer ratios will also be presented.

Index Terms — Ultra-wideband (UWB) radio, RF front-end, LNA, phase-splitter, NF, SIR, transmission lines, power-match, un-match, voltage-boost.

I. INTRODUCTION

Since the FCC's First Report and Order on ultra-wideband (UWB) communications in 2001 [1], UWB signaling has become an increasingly popular method of wireless data transmission. To transmit and receive signals that span greater than 500MHz invokes new challenges for the design and implementation of such a system. For the analog front-end, the challenge of following RF tradition to achieve power-match and low noise figure (NF) becomes a difficult task due to the broad bandwidth. Simple L - or T -shaped matching structures are unusable due to their reliance on narrowband, high Q approximations for impedance transformation. Wideband LC ladder-matching structures become unwieldy because of the large LC values required for operation in the baseband UWB frequencies of interest. However, noisy resistor-based matching structures and active matching techniques are good candidates for achieving a power match for the baseband UWB bandwidth [2]-[3]. Finally in addition to the efforts made on achieving power match for LNAs over the UWB frequency band of interest, there has also been theoretical work done on improving noise figure of UWB LNAs by ignoring power matching in order to have freedom to directly match for low noise figure [4].

This paper presents a baseband pulse-based BPSK UWB front-end that is a component of a system-on-a-chip transceiver that achieves wireless transmission at 200kbps . Section II presents matching technique theory for the low-noise amplifier (LNA), transmission (TX) line effects, and

their effect on NF and UWB signal to sinusoidal interferer ratio (SIR). Section III outlines the design of the front-end. Finally, Sections IV and V present measured results and conclusions.

II. UWB FRONT-END MATCHING THEORY

Traditionally, source and load impedances of a TX line are matched to the characteristic impedance of the TX line to acquire maximum power transfer and minimize reflections. However, the benefits of matching should be revisited for pulsed UWB systems.

A. Benefits of an Un-Matched Network

Achieving maximum power transfer from the antenna to the LNA input through a TX line may not be optimal for a pulsed UWB signal. Since a common source LNA is a voltage-controlled current source, maximizing the input voltage rather than the power creates the largest output current. This implies that an infinite input impedance is desired for such an LNA. The reflection coefficient, Γ_L , of such an LNA is 1. This particular case of an un-matched network will be called the voltage-boosted case.

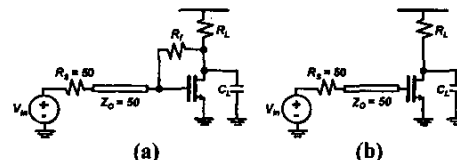


Fig. 1. (a) Power-matched and (b) voltage-boosted LNAs.

Two wideband LNAs are shown in Fig. 1. The power-matched LNA (a) uses a well-known, wideband matching technique. The input impedance of this LNA in the passband is $R_g/A_v=50\Omega$. $|\Gamma_L|=0$ for the power-matched case, and the LNA produces a total gain for a pulse of $(1+\Gamma_L) \cdot A_v=A_v$. By removing R_g as shown in the voltage-boosted LNA (b), the input is terminated only by the gate capacitance. $|\Gamma_L|=1$ for the voltage-boosted case, and the LNA produces a total gain for a pulse of $(1+\Gamma_L) \cdot A_v=2 \cdot A_v$. The voltage-boosted LNA gain is increased by 6dB if loading effects from R_g are ignored. This 6dB comes from a reflection at the input to the LNA. In addition to the noiseless gain, the drain noise contribution from the MOSFET is unchanged. These combined effects improve the NF of the voltage-boosted LNA.

B. Tradeoffs of an Un-Matched Network

By not matching the LNA input, reflections are introduced into the system. For pulsed UWB signals, these reflections appear as echoes of the pulse at the LNA input. Under constraints that depend on the echo delay time and the algorithms in the RAKE receiver, these echoes can be ignored or partially recovered for signal detection.

A major concern for UWB systems is coexistence with narrowband interferers. Unlike the echoes of UWB pulses, a steady-state sinusoidal interferer forms a non-unity voltage-standing-wave-ratio (VSWR) in an un-matched regime with maximum and minimum amplitudes that are correspondingly larger and smaller than when matched. This appears as a frequency-dependent degradation or improvement of SIR relative to the power matched case.

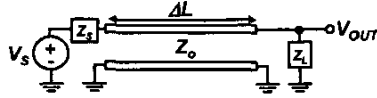


Fig. 2. Simulation setup for TX line.

Simulations are performed using the setup in Fig. 2 to determine how standing waves at the LNA input affect SIR. As the interferer frequency is swept within the UWB band at fixed TX line lengths (ΔL) and Γ 's, the standing wave amplitude at the LNA input varies between a minimum and a maximum value, depending only on $|\Gamma_L \cdot \Gamma_S|$. The frequencies at which the maxima and minima occur depend on the phases of Γ_L and Γ_S , ΔL , and properties of the TX line.

The theoretical maximum and minimum amplitudes of the standing wave are shown in (1) and (2) with respect to Fig. 2.

$$V_{\max} = V_I L (1 + \Gamma_L) (1 - L^2 |\Gamma_S \Gamma_L|)^{-1} \quad (1)$$

$$V_{\min} = V_I L (1 + \Gamma_L) (1 + L^2 |\Gamma_S \Gamma_L|)^{-1} \quad (2)$$

where

$$V_I = V_S Z_o (Z_o + Z_s)^{-1} \quad (3)$$

L is the loss through the cable. The number of round-trip reflections N for standing waves to achieve 98% of the final value is calculated using (4), and the time for this to occur, τ_{98} , is calculated in (5). ϵ_r is relative permittivity of the TX line and c is the speed of light.

$$N = -1.6989 (\log_{10} (L^2 \Gamma_S \Gamma_L))^{-1} - 1 \quad (4)$$

$$\tau_{98} = 2N \cdot \Delta L \cdot \sqrt{\epsilon_r} \cdot c^{-1} \quad (5)$$

N and τ_{98} help to specify the length and resolution of the RAKE receiver. Also, if $1/\tau_{98}$ is much greater than the interferer symbol rate, it is reasonable to assume the modulated interferer behaves mostly like a pure tone.

Fig. 3 is a plot using the system shown in Fig. 2 of the maximum and minimum changes in SIR at V_{out} vs. $|\Gamma_L \cdot \Gamma_S|$, where the SIR at V_s is at 0dB. The SIR for any sinusoidal

interferer within a given $|\Gamma_L \cdot \Gamma_S|$ matching environment lies within the boundaries of the two curves at $|\Gamma_L \cdot \Gamma_S|$.

A typical antenna $|S_{11}|$ of $-10dB$ corresponds to a Γ_S magnitude of 0.3. The reflection coefficient of the voltage-boosted LNA in Fig. 1 is 1 (capacitor termination). The product of $|\Gamma_L \cdot \Gamma_S|$ is 0.3. Therefore, from Fig. 3, the worst-case change in SIR is a decrease of $3dB$, and the best-case change is an improvement of $2.2dB$, due to amplification and attenuation of the sinusoidal interferer, respectively.

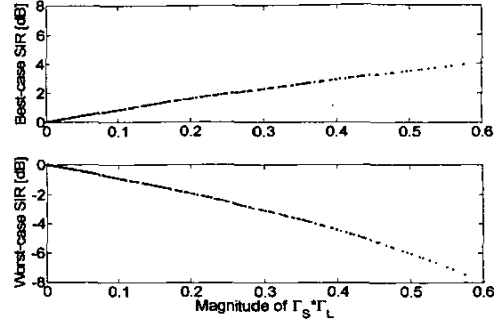


Fig. 3. Simulated best- and worst-case change in SIR for un-matched load and source.

III. BASEBAND UWB FRONT-END DESIGN

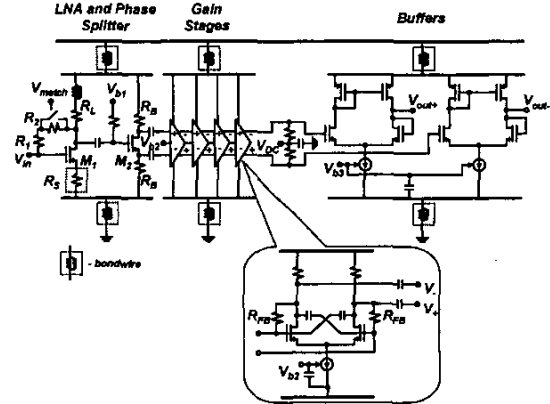


Fig. 4. Front-end circuits.

The wideband pulse-amplifying front-end is shown in Fig. 4. The LNA is based upon a traditional wideband feedback amplifier topology [5] and incorporates inductor peaking for bandwidth extension [6]. A modification upon the feedback resistor network allows this LNA to operate in two broadband matching modes: power-matched and voltage-boosted. To achieve broadband power-matching to an antenna with $|S_{11}| < -10dB$, the NMOS switch controlled by V_{MATCH} is closed and R_2 is shorted. To achieve the voltage-boosted case where Γ_L approaches one, the switch is opened.

The gain and input impedance of the power-matched and voltage-boosted cases are shown in the equations below.

Power-matched, for input V_i in (3):

$$A = g_m \cdot (R_L // R_1)(1 + g_m \cdot R_S)^{-1} \quad (6)$$

$$Z_{LNA} = R_1 \cdot A^{-1}. \quad (7)$$

Voltage-boosted, for input V_i in (3):

$$A = g_m \cdot (1 + \Gamma_L)(R_L // (R_1 + R_2))(1 + g_m \cdot R_S)^{-1} \quad (8)$$

$$Z_{LNA} = (R_1 + R_2) \cdot A^{-1}. \quad (9)$$

For the voltage-boosted case, R_2 is two orders of magnitude larger than R_1 . The input shunt impedance created by C_{gs} , the bondpad, and PCB is designed to be larger than Z_O through the bandwidth of the amplifier. Thus, Γ_L approaches one. This gives the maximum noiseless voltage amplification, which is $(1 + \Gamma_L) \approx 2$ times the power-matched case. R_1 and R_2 allow M_1 to be self-biased in both modes of matching.

The LNA is followed by a phase-splitter to convert the single-ended wideband RF signal to a fully-differential signal. The current through the R_B resistors and transistor M_2 are equal, thereby allowing equivalent magnitude gain to appear at the source and drain of transistor M_2 .

Cascaded gain stages thereafter are AC -coupled and individually self-biased with R_{FB} to avoid parasitic feedback paths through the signal and biasing paths. These gain stages have cross-coupled series capacitors to extend bandwidth. The gain of the front-end can be adjusted externally through V_{b2} . The buffers are operational g_m -amplifiers configured in unity gain and AC -coupled, with a configurable output DC bias.

The power supply network is separately grouped and isolated to avoid oscillations that can arise through it. Since this is a pulse-amplifying front-end, it must be non-dispersive, thereby possessing flat gain and constant group delay through the frequency range of interest.

IV. MEASURED RESULTS

A. UWB Front-End IC Results

Fig. 5 shows S_{21} , NF, S_{11} , and group delay under both matching conditions. A voltage gain increase of less than $6dB$ from the power-matched case to the voltage-boosted case is observed, because $\Gamma=0.39$ in the power-matched case, due to an underestimated source impedance of the LNA. This also degrades the NF from simulation results.

For the voltage-boosted case, the average NF decreases from $10.2dB$ to $7.9dB$ and the gain increases from $38dB$ to $42dB$. The front-end consumes $71mW$ of power for both configurations. Fig. 6 is a die photo of the front-end.

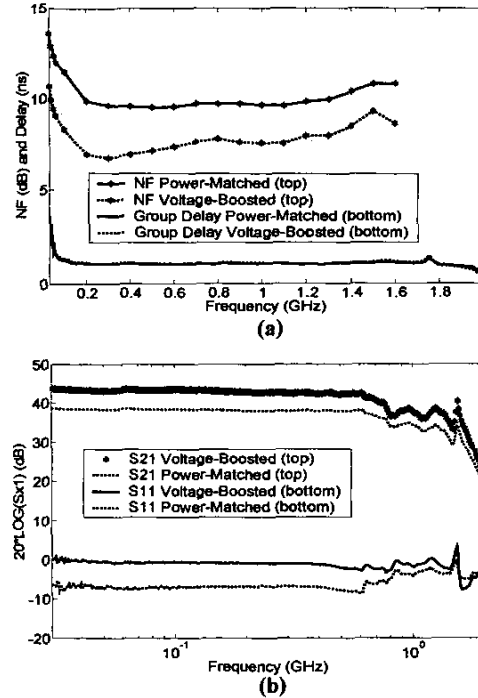


Fig. 5. Measured (a) NF, group delay, (b) S_{11} and S_{21}

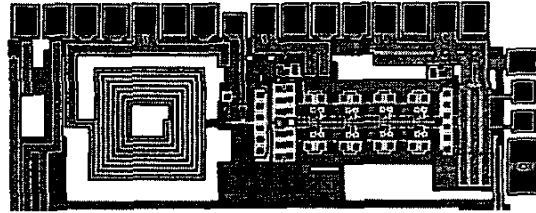


Fig. 6. Die photo.

B. TX Line and Matching Effects on Pulses and Sinusoidal Standing-Wave Based Signals

For pulse-based input signals, it is possible to observe various echoes following the initially received transient pulse at multiples of

$$\Delta\tau = 2 \cdot \Delta L \cdot \sqrt{\epsilon_r} \cdot c^{-1}, \quad (10)$$

if Γ_L and Γ_S are both non-zero. A representation of the measurement setup is shown in Fig. 7.

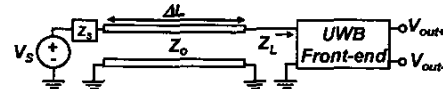


Fig. 7. Matching network TX line measurement setup.

Z_S and V_S represent the antenna source impedance and source voltage, respectively. ΔL is set to $100cm$ in order to observe reflections, and ϵ_r , relative permittivity, is 2, thereby fixing $\Delta\tau = 9.5ns$. Fig. 8 shows the six different

combinations of Z_L in power-matched and voltage-booster conditions vs. $|Z_S| = Z_o$, $|Z_S| < Z_o$, and $|Z_S| > Z_o$. The magnitude of source mismatch is constrained by $|S_{11}| = 20 \cdot \log_{10} |(Z_S - Z_o)/(Z_S + Z_o)| < -10 \text{ dB}$, thereby restricting Z_S to 25Ω and 100Ω. For $Z_S = 100\Omega$, the echoes are the same sign as the primary pulse. However, for $Z_S = 25\Omega$, the echoes have alternating sign, due to a negative Γ_S . As stated before, these pulse echoes and inversions can be partially recovered in the digital back-end RAKE receiver. As for the UWB pulse magnitudes, the largest Γ_L -dependent voltage gain comes from the voltage-booster mode with a 25Ω source mismatch.

For the sinusoidal standing-wave based input signals, the same testing configuration shown in Fig. 7 is used. The resulting min and max standing wave amplitudes are shown in Fig. 9. The legend in Fig. 9 includes the associated output pulse magnitude per sinusoid matching condition. The input pulse amplitude for Fig. 8 and input sinusoid amplitude for Fig. 9 are equivalent. The dotted lines in Fig. 9 serve only to visually connect the max and min values of a given series. The max and min amplitudes occur at multiples of $0.5 \cdot \Delta\tau^{-1}$ in frequency. As seen from the data, the standing wave is prevented from growing larger than its input amplitude and additionally degrading the SIR if the source is matched as close to Z_o as possible.

V. CONCLUSIONS

Theoretical and experimental results of a baseband UWB front-end have been presented. Tradeoffs of a matched and un-matched LNA input impedance were discussed. Strictly for UWB pulses, it is always beneficial to un-match the LNA input if the electrical delay in the cable is longer than the pulse. This improves the gain and NF of the LNA. In the presence of a narrowband interferer, SIR can be improved or degraded (relative to the power matched case) when un-matched, depending on parameters of the system. This creates an opportunity for co-design of the LNA and antenna, such that SIR is improved at frequencies where known interferers impact the system, and degraded in unused frequency bands. If the antenna is sufficiently close to the LNA such that TX line theory can be ignored, then the un-matched network achieves an improvement in NF without SIR fluctuations.

ACKNOWLEDGEMENTS

This research is sponsored by Hewlett-Packard under the HP/MIT Alliance and the National Science Foundation under contract ANI-0335256. Any opinions, findings, and conclusions or recommendations expressed in this material are those of the authors and do not necessarily reflect the views of the National Science Foundation.

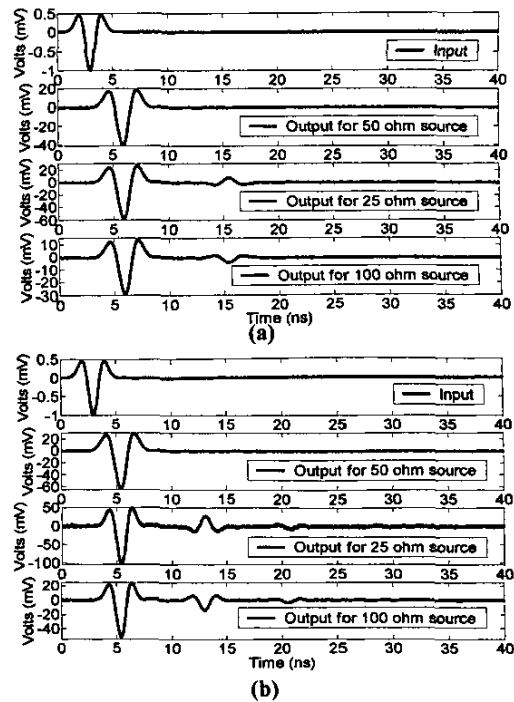


Fig. 8. Measured (a) power-matched and (b) voltage-booster pulse waveforms.

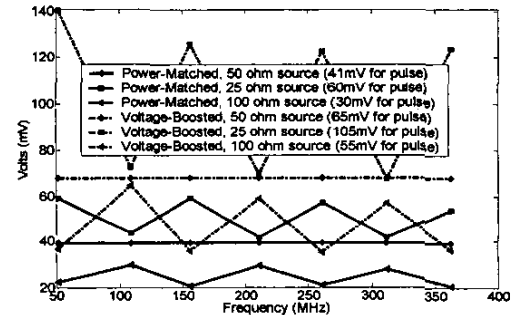


Fig. 9. Measured sinusoidal max and min standing wave amplitudes vs. frequency (data valid only at corners of plot).

REFERENCES

- [1] Federal Communications Commission, *Ultra-Wideband (UWB) First Report and Order*, February 2002.
- [2] F. Bruccoleri, E.A.M. Klumperink, B. Nauta, "Noise canceling in wideband CMOS LNAs," *ISSCC Dig. Tech. Papers*, vol. 1, pp. 406-407, February 2002.
- [3] C. Bowick, *RF Circuit Design*, Newnes, 1997.
- [4] J. Lerdworatawee, W. Namgoong, "Low Noise Amplifier Design for Ultra-Wideband Radio," *Proceedings of the 2003 ISCAS*, vol. 1, pp. I-221-I-224, May 2003.
- [5] H. Knapp, et. al., "15GHz Wideband Amplifier with 2.8dB Noise Figure in SiGe Bipolar Technology," *RFIC Symposium Digest*, pp. 287-290, 2001.
- [6] T. H. Lee, *The Design of CMOS Radio-Frequency Integrated Circuits*, Cambridge University Press, 1998.